Hybrid Geothermal-Biomass Power Plants: Applications, Designs and Performance Analysis

Ian Thain and Ronald DiPippo

12 Raven Grove, Havelock North, Hawkes Bay, New Zealand and 16 Bay View Ave., S. Dartmouth, MA, USA

I.a.thain@xtra.co.nz and rondipippo@comcast.net

Keywords: geothermal, biomass, hybrid, power cycles, optimization, efficiency, forestry waste, New Zealand

ABSTRACT

Hybrid fossil-geothermal power plants have been proposed and studied in detail for nearly one hundred years. This paper reviews the concept of superheating geothermal steam by means of a forest wood waste combustion plant. New Zealand is studied as a promising country for such plants owing to the large sustainable forestry industry and the close proximity of numerous geothermal resources.

The Rotokawa I geothermal plant is used as a case study for a hypothetical biomass-geothermal hybrid plant. The original plant, a 29 MW flash-binary combined cycle was augmented by the addition of a biomass-fired superheater inserted in the main steam-line from the cyclone separator to the steam turbine. The brine from the separator was maintained but the steam expanding under dry conditions on exiting the back-pressure turbine was able to provide additional heat to two of the bottoming binary cycles. Owing to the superheat in the steam significantly more power may be generated and the expansion is completely dry allowing a higher turbine isentropic efficiency. The case study shows the hypothetical hybrid Rotokawa I plant out-generates the basic plant by 8,548 kW, a 32% gain, with 6,911 kW coming as additional output from the back-pressure steam turbine, and the rest coming from the two steam-condensate-heated binary units. Since the plant receives 19,330 kWt from biomass combustion, the extra power output may be seen as using the biomass heat with a thermal efficiency of 0.442, much higher than a conventional biomass power plant. The Second Law or exergy efficiency of the hybrid plant is comparable to that of the basic geothermal plant, but somewhat lower owing to the large temperature difference in the biomass superheater.

Three more biomass-geothermal hybrid schemes are proposed and studied. System I is a double-flash geothermal plant that uses biomass energy to enhance its performance. System II consists of a single-flash geothermal plant coupled to a biomass plant superheater that delivers superheated steam to a geothermal turbine, with geothermal brine used for feedwater heating for the biomass plant. System III is mainly a biomass power plant that takes advantage of geothermal energy to enhance its performance. All three systems exhibit advantages in terms of net power generated relative to individual plants. System III was optimized for best efficiency and highest power for a given geothermal resource.

The paper also includes a survey of the forest waste in New Zealand regarding its availability, cost and combustion properties. The engineering challenges facing the designer of hybrid biomass-geothermal plants are presented and discussed.

1. INTRODUCTION

The earliest hybrid fossil-geothermal plant was proposed in 1924 by Coufourier [DiPippo, 1978]. The use of geothermal liquid for feed water heating in an otherwise conventional fossil-fueled power plant was suggested as long ago as 1961[Hansen, 1961], and fossil superheating of geothermal steam was described nine years later [Bruce, 1970; James, 1970]. A variety of hybrid fossil-geothermal power systems were studied extensively by the Brown University research group starting in the late 1970s [Kestin et al, 1978; Khalifa et al, 1978; DiPippo et al, 1979; DiPippo and Avelar, 1979]. Among the kinds of plant examined were geothermal preheat systems in which low-to-moderate geothermal liquids are used to replace extraction steam and provide feedwater heating; fossil superheat systems in which a fossil fuel, ideally natural gas, is fired to add superheat to geothermal steam prior to entering the turbine; and various combinations of these ideas. All of these studies indicated that hybrid systems outperform two separate power systems with the same energy inputs, with the size of the advantage determined by the configuration of the hybrid system. The economic feasibility of the hybrid system depends strongly on how close the two energy sources are to each other.

Recently the MIT energy research group studied several conceptual hybrid solar-geothermal designs [Manente et al, 2011]. A geothermal binary plant and a solar photovoltaic array share a plant site at Stillwater, Nevada [ENEL, 2011].

The concept of a geothermal-biomass hybrid plant has not been elaborated in the literature so far, despite the fact that such a plant has been operating near Honey Lake in California since 1989 [*Geothermal Hot Line*, 1988]. An engineering and economic report on the Honey Lake plant served as a feasibility study and is available on-line [Morrison-Knudsen, 1982].

The basic notion of a hybrid biomass-geothermal power plant is shown in the simple diagram Figure 1.
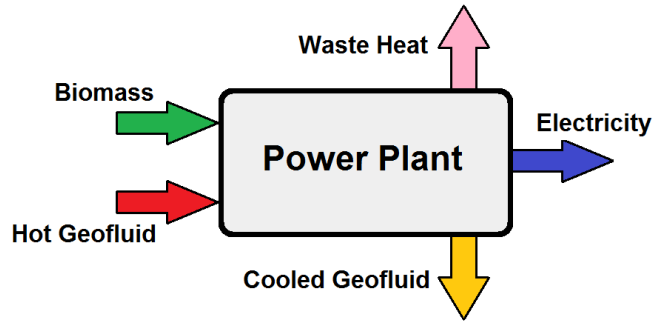
Figure 1: Generalized hybrid system schematic.

Biomass in the form of waste forestry product is fired with air to produce hot flue gases that are used to raise steam for a steam turbine and generate electricity. Hot geothermal fluid usually in the form of hot liquid under pressure also enters the plant. How these two input streams interact depends on the particular design of the cycle. Besides electricity, waste heat and cooled geofluid must be discharged from the plant. From an exergy point of view, the input exergy from the biomass and the geofluid power the plant and the ratio of the output electricity to the sum of the inputs is the utilization efficiency. The thermal efficiency for the plant is not well-defined thermodynamically since the geofluid undergoes a series of processes, not a closed cycle. These will be explored in detail, first with an example using an actual geothermal plant and then with several conceptual designs.

2. APPLICATION OF THE CONCEPT TO ROTOKAWA I PLANT, NEW ZEALAND

As a simple hypothetical example of how a hybrid geothermal-biomass plant might be configured and perform, consider the case of the first geothermal plant at Rotokawa on New Zealand's North Island [Lind et al 2013]. Figure 2 is an aerial view of the power station from Google Earth as of April, 12, 2012. The steam-brine binary unit, added later, was not part of the original configuration and was not included in the hypothetical study reported in this paper.
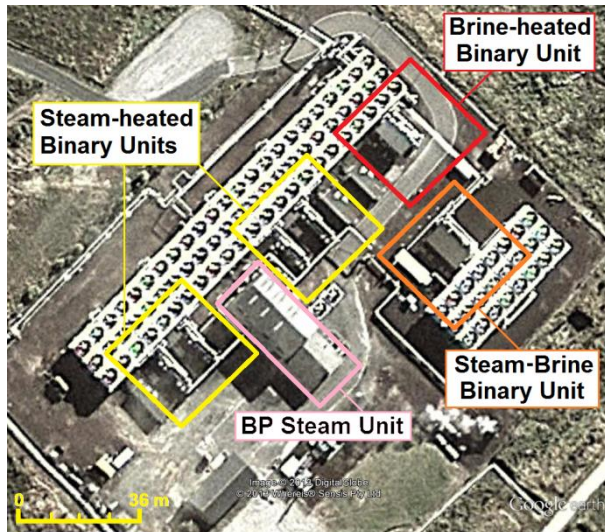

Figure 2: Aerial view of Rotokawa power station. [*Google Earth*, 4/12/2102]

Figure 3 shows a simplified flow diagram of the original plant, the 29 MW (nom.) Rotokawa I [Legmann, 1999], modified and augmented by the addition of a hypothetical biomass-fired superheater (BM-SH). The original plant was a combined flash-binary system. Two-phase geofluid received via two wells (RK5 & RK9) from the reservoir is separated in a cycle separator (CS), with the steam being delivered to a 14 MW (nom.) back-pressure steam turbine (ST) and the brine being sent to the heat exchangers of a 5 MW (nom.) binary unit. The steam exhausted from the steam turbine is used as the heating medium for two more 5 MW (nom.) binary units. All geofluid is reinjected via three wells (RK1, RK11 & RK12). The working fluid for all binary cycles is normal-pentane.

For this simple example of biomass hybridization, a superheater in inserted in the main steam line from the cyclone separator and the steam turbine, the biomass superheater (BM-SH); see Figure 3. Only the inlet and outlet states of the steam turbine are affected with this change, relative to the original plant. In the original plant, states 4 and 4' are identical.

The process diagram in temperature-entropy coordinates is given in Figure 4, showing the plant specifications and processes before and after hybridization for the actual resource conditions at Rotokawa and reasonable conditions for the hybrid plant.
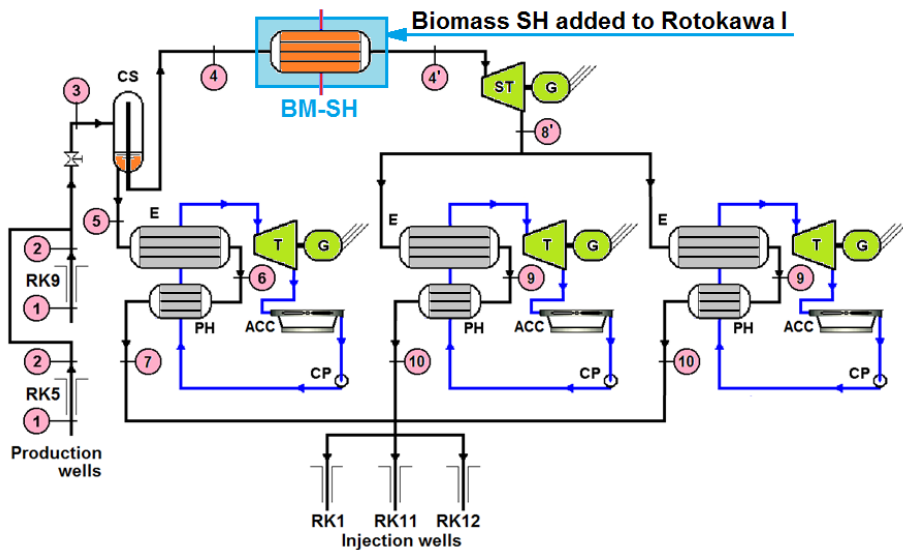
Figure 3: Hypothetical Rotokawa I hybrid geothermal-biomass power plant, modified from [Legmann, 1999].
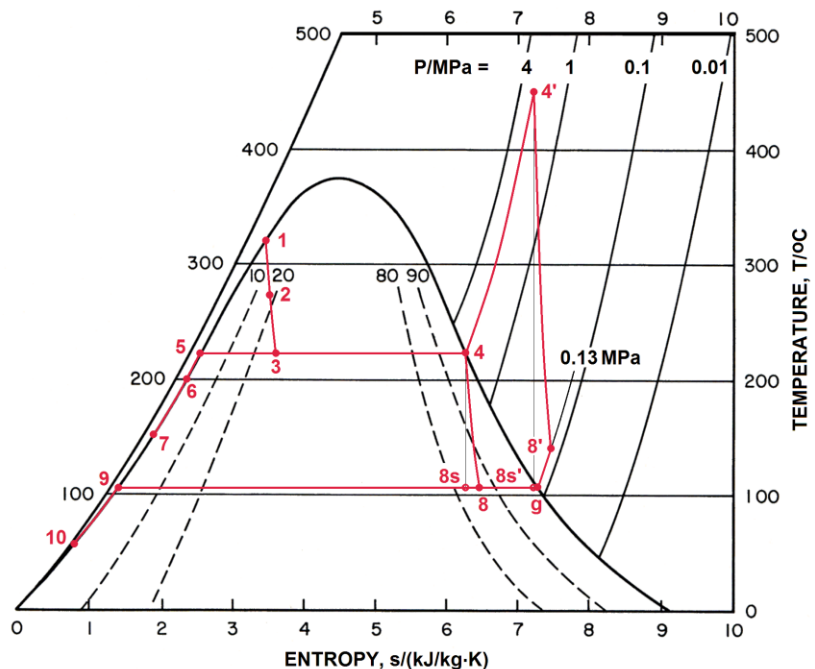

Figure 4: Steam and water processes for Rotokawa I basic and hybrid plants. Note: Basic plant uses processes 1-2-3-4-5-6-7-8-9-10; Hybrid plant uses 1-2-3-4-4'-5-6-7-8'-g-9-10; State g represents the saturated vapor at the turbine exhaust pressure.

The process diagrams for the bottoming binary cycles are not included since they are minimally affected by the change to a hybrid system. The two units fed with exhaust steam will receive more heat in the hybrid case because of the superheat in the turbine exhaust (state 8', Figure 4) and thus will generate more power than the base plant.

The power from the steam turbine in the base case is found from:

$$\dot{W}_{ST} = \dot{m}_4 (h_4 - h_8)$$

(1)

where

$$\dot{m}_4 = x_3 \dot{m}_1 = [(h_3 - h_5)/(h_4 - h_5)]\dot{m}_1$$

(2)

If the geofluid does not flash in the formation, the enthalpy at states 1, 2 and 3 may be assumed equal. This allows the quality at state 3, i.e., the steam fraction that enters the turbine, to be determined from the reservoir condition and the flash pressure or temperature. If the geofluid does flash in the formation, the quality at state 3 will be higher than this (the so-called "excess enthalpy" effect) and will need to be found from wellhead measurements.

For the original plant, with reference to Fig. 4, it can be seen that the turbine expansion process is wet. The enthalpy of the steam leaving the turbine, h_8, may be found with the aid of the Baumann rule on the assumption that the turbine would have an isentropic efficiency of, say 85%, for a completely dry expansion process. Thus, the following equation was used to find h_8 [DiPippo, 2012a]:

$$h_8 = \frac{h_4 - A[1 - h_9/(h_g - h_9)]}{1 + A(h_g - h_9)}$$

(3)

where

$$A = 0.5\eta_{TD}(h_4 - h_{8s}) = 0.425(h_4 - h_{8s})$$

(4)

For the hybrid plant, the enthalpy at turbine exhaust state, $h_{8'}$, since the expansion is completely dry, may be found from the simple equation

$$h_{8'} = h_4 - \eta_{TD}(h_4 - h_{8s'})$$

(5)

using $\eta_{TD} = 0.85$. The mass flow rate of biomass was found by an overall energy balance of the superheater, namely,

$$\dot{Q}_{SH} = \dot{m}_{bio}(HHV) = \dot{m}_4(h_{4'} - h_4)$$

(6)

Equation (6) assumes an ideal superheater, i.e., no heat losses. Assuming, say, a 75% efficient BM-SH, then the biomass burn rate can be found from:

$$\dot{m}_{bio} = \dot{m}_4(h_{4'} - h_4)/(0.75 \times HHV)$$

(7)

No attempt was made to design the biomass superheater. Whereas the design of a conventional superheater is well known and such systems are commercially available, no company, to the authors' knowledge, supplies a system to superheat saturated geothermal steam using direct hot combustion gases in excess of 950°C obtained from the firing of forest residue.

An Excel spreadsheet was written that incorporated RefProp [NIST, 2013] as a subroutine to carry out the analysis of the two plants; the results are summarized in Tables 1 and 2. Note that a plant parasitic power of 2.5 MW was assumed for both cases.

Table 1. Summary of heat and work performance for basic and hybrid plants.

Basic Plant		Hybrid Plant	
Heat Input Terms			
Brine cycle, kWt	27,957	Brine cycle, kWt	27,957
Steam cycles, kWt	77,138	Steam cycles, kWt	91,994
Total heat, kWt	105,095	Biomass heat, kWt	19,330
		Total heat, kWt	139,281
Power Terms			
Steam turbine, kW	14,035	Steam turbine, kW	20,946
Brine cycle, kW Net	5,161	Brine cycle, kW Net	5,161
Steam cycles, kW Net	10,163	Steam cycles, kW Net	11,799
Total – 2,500, kW Net	26,858	Total – 2,500, kW Net	35,406
Plant Efficiencies			
Thermal efficiency	0.256	Thermal efficiency	0.254

The thermal efficiency is the ratio of the total net power output to the rate of heat input from the geofluid brine and steam condensate (basic plant), plus the burning of the biomass (hybrid plant). This is not strictly in accordance with the usual definition of thermal efficiency since the steam turbine is not part of a closed cycle. The characteristics of the forest residual wood waste are discussed below in Sect. 3. The biomass fuel burn rate is 1.26 kg/s (ideal BM-SH) or 1.68 kg/s (75% BM-SH).

The thermal efficiencies for the closed binary cycles, defined as the ratio of the net cycle power output to the thermal power input, are 0.132 for the two steam-condensate heated cycles and 0.185 for the brine-heated cycle. The latter value may seem high for a binary cycle but the brine temperature, T_5, is much higher than is usually found in binary plants, namely, 224°C. Furthermore, these

do not account for other plant parasitic power requirements. It is seen that the plant thermal efficiency, as defined here, turns out to be about the same for the basic and hybrid cycles. The hybrid plant, however, out-generates the basic plant by 8,548 kW, a 32% gain, with 6,911 kW coming as additional output from the back-pressure steam turbine, and the rest coming from the two steam-condensate-heated binary units. Since the plant receives 19,330 kWt from biomass combustion, the plant extra power output may be seen as using the biomass heat with a thermal efficiency of 0.442, an impressive conversion efficiency. The incremental thermal efficiency of the steam turbine is 0.358, i.e., the ratio of the increase in steam turbine power output to the rate of biomass heat input.

Table 2. Summary of exergy performance for Rotokawa I basic and hybrid plants.

Basic Plant		Hybrid Plant	
Exergy Input			
Geofluid - reservoir, kW	60,144	Geofluid - reservoir, kW	60,144
Geofluid - fence, kW	55,815	Geofluid - fence, kW	55,815
		Biomass:	
		Specific exergy, kJ/kg	16,500
		Exergy, kW	20,778
		Total - reservoir, kW	80,922
		Total - fence, kW	76,592
Power Output			
Net electric power, kW	26,858	Net electric power, kW	35,406
Utilization Efficiencies			
Based on reservoir	0.447	Based on reservoir	0.438
Based on fence	0.481	Based on fence	0.462

An assessment based on exergy provides a useful picture of system performance [Moran, 1989; DiPippo and Marcille, 1984; DiPippo, 2012b]. The power output is compared to the input exergy supplied by the geofluid and the biomass. The specific exergy of the biomass was taken as 16,500 kJ/kg, an average of values found in the literature for wood waste [Wall, EOLSS; Dias and Perrella, 2004]. The results are presented in Table 2.

For the basic plant, only the incoming geofluid exergy matters; two values are given, one for the reservoir condition and one at the "fence" location. If the plant and field are owned by the same entity, the former is a better basis, whereas if they are owned by separate entities, the latter is a better basis from the point of view of the plant owner who buys the fuel (and its exergy) from the field owner. The utilization efficiencies are impressive for both cases, but the hybrid plant shows a somewhat lower efficiency owing to exergy losses in the BM-SH caused by the very large temperature difference between the combustion gases and the geothermal steam.

3. BIOMASS FUEL CONSIDERATIONS

Whereas other forms of fossil fuels could be used for this hybrid power generation concept, by utilizing waste biomass as the combustion fuel, the power plant can be a sustainable, renewable and benign source of electrical generation. However, close proximity of both geothermal and biomass resources are required to make this an economically viable power generation option. Much of New Zealand's North Island is suitable, and similar conditions are likely to exist in Indonesia, the Philippines, and other geothermal-rich countries where climatic conditions support the rapid growth of biomass crops.

The co-location requirement is often an important limiting factor in determining the feasibility of a conceptual hybrid plant. Bruce [1970] ruled out adding superheat to the steam at The Geysers field in California at that time because of the cost of bring fuel to the plant site. However, for a biomass wood-waste/geothermal plant situated in New Zealand, there are abundant energy resources of both kinds in close proximity on the North Island. Figure 5 identifies several geothermal power stations and the Kaingaroa Forest, which at 2,900 km[2] is the largest plantation in the southern hemisphere [McKinnon, 2012]. The forest consists predominantly of Monterey pine trees (*pinus radiata*) with lesser amounts of Douglas fir and other species, which are harvested on a sustainable basis, creating a continuous supply of biomass in the form of forest residue wood waste [Kaingaroa Timberlands, 2013; *Wikipedia*, 2013; Roche, 2012].

The type and chemical/physical properties of the wood waste for any particular application will determine the heat release from combustion and the required mass flow of fuel to supply a hybrid plant of a given rating. Forests that are maintained sustainably often consist of conifers such as Douglas fir and various types of pine. Figure 6 [Ciolkosz, 2010] shows the heating values for Douglas fir and pine: the dry values are shown in the detail box and the effect of moisture content in the main graph. For a variety of typical wood wastes, Ciolkosz [2010] shows that the HHV of forest woods range from about 18,600-22,400 kJ/kg (dry), or 13,300-17,100 kJ/kg (25% moisture). It may be seen that the moisture content is far more influential in determining the heating value than the particular species of wood.

Currently in New Zealand it is common practice to leave the forest residue on the ground during clear-cutting operations. The collection and burning this waste is recognized as a carbon neutral process, and clearing the ground allows for easier and quicker re-planting of the forest. Thus the proposed utilization method is environmentally benign.

The logistics and cost of gathering wet forest residue in the Greater Wellington region in New Zealand were studied in 2009 [NZCEC, 2009]. When the forest residue was gathered at the time of logging and transported over an average distance of 30 km, the cost of this operation was reported to be NZ$3.20/GJ. The calorific value of the forest residue had average value of 8 GJ/t. Thus biomass fuel in this form delivered to a power plant was estimated to cost NZ$25.60/t. Including power plant-site chipping, hogging and possibly drying of the received biomass was estimated to add another NZ$10/t, resulting in a burnable fuel cost of around NZ$35-40/t. These costs may be converted to 2009 US dollars using the exchange rate in June 2009: 1 NZ$ = 0.6386 US$ [X-Rates, 2009].

For this hypothetical Rotokawa hybrid study, the Kaingaroa Forest of New Zealand has been posited and the trees assumed to be Monterey pine; the higher heating value HHV was taken to be 15,350 kJ/kg. This HHV value assumes 25% moisture in the biomass. The mass flow of biomass to the furnace needed to supply the superheat described in Sect. 2 is 1.26 kg/s from Eq. (6) for an ideal furnace and 1.68 kg/s from Eq. (7) for a 75% efficient furnace. At the latter fuel rate for the hybrid Rotokawa plant, assuming 80% capacity factor, the average annual biomass fuel cost would be between 2.5 and 2.8 NZ¢/kWh, based on the incremental power output from the combustion of the biomass. Plant design should be based on measured heating values for the particular biomass that is available in the neighborhood of the plant.
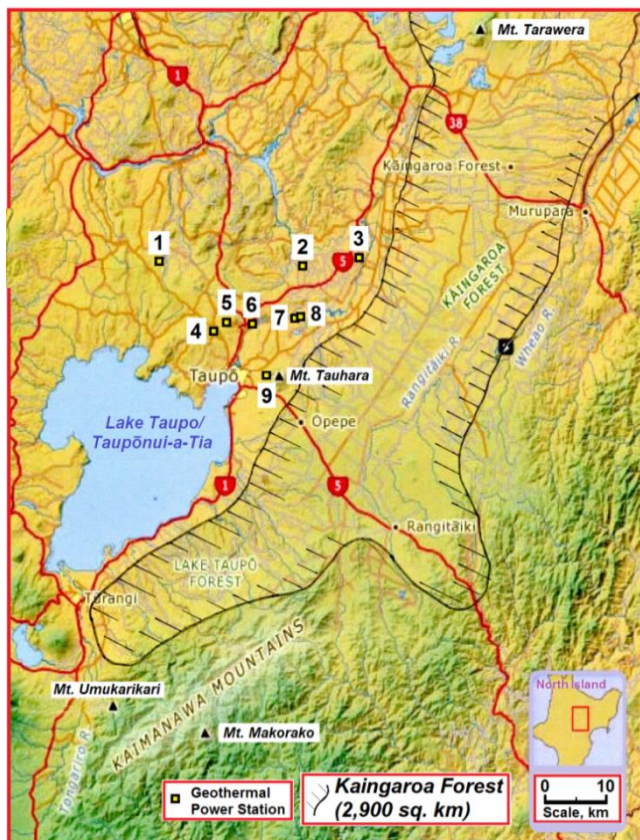
Figure 5: A portion of New Zealand's North Island illustrating the co-location of geothermal power plants and the southern part of the Kaingaroa Forest, after [McKinnon, 2012]. Power plants: 1-Mokai I & II, 95 MW; 2-Ngatamariki, 80 MW; 3-Ohaaki, 65 MW; 4-Poihipi, 55 MW; 5-Te Mihi, 159 MW; 6-Wairakei, 132 MW; 7-Taonga (Nga Awa Purua), 140 MW; 8-Rotokawa, 32 MW; 9-Te Huka, 23 MW.
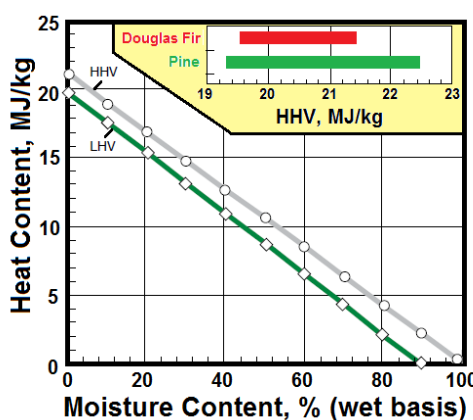
Figure 6. Higher heating value for biomass (Douglas fir and pine), after Ciolkosz [2010].

As a final thought on this subject, in arid regions which have geothermal resources and good solar conditions, geothermal steam condensate can be used to provide a reliable source of irrigation water to support the growth of coppice biomass fuel crop (CBF), typically poplar and willow. CBF can be harvested on a 3-year rotational basis with the ground root stock able to sustain multiple harvesting cycles without the need for replanting. Geothermal regions such as the Salton Sea in the USA and Olkaria in Kenya are places where condensate-irrigated coppice crops could be grown to support a sustainable geothermal-biomass hybrid power plant. Already at Olkaria residual biomass is available from the vast flower growing operations in the area, which if combined with CBF could make the hybrid concept a viable proposition for this huge geothermal area.

4. CONCEPTUAL DESIGN DESCRIPTIONS

A geothermal-biomass hybrid power plant can take various forms. One conceptual version is essentially a biomass-fueled power plant with a geothermal assist, whereas an alternative version is the opposite, namely, a geothermal flash plant with a biomass boost. The choice between the two basic concepts will turn on the site-specific conditions for the particular application. Detailed differences for each of the basic conceptual designs may be used to match the plant to the energy resources.

In this section we present three conceptual designs including a minor variation of one of them. We begin with System I, which falls into the latter version, namely, a double-flash geothermal plant that uses biomass energy to enhance its performance. The next one is a fairly complex system, System II, which merges a single-flash geothermal plant with a biomass power plant into a kind of compound hybrid system [DiPippo & Avelar, 1979]. The last one, System III, is mainly a biomass power plant that takes advantage of geothermal energy to enhance its performance. A slight variation of the last design is also discussed.

4.1 System I - Biomass-Enhanced Geothermal Double-Flash Plant

System I shown in Figure 7 is fundamentally a geothermal double-flash plant that is assisted by heat from a biomass resource. The high-pressure separated geosteam is first superheated in the biomass furnace. Then after powering the high-pressure stages of the turbine is mixed with the low-pressure separated steam and returned to the furnace for reheating prior to entering the low-pressure stages of the turbine. The still hot brine leaving the low-pressure separator is used to preheat the combustion air and assist in drying the biomass fuel prior to admission to the furnace.

A summary of the performance of this system is given in Sect. 5.
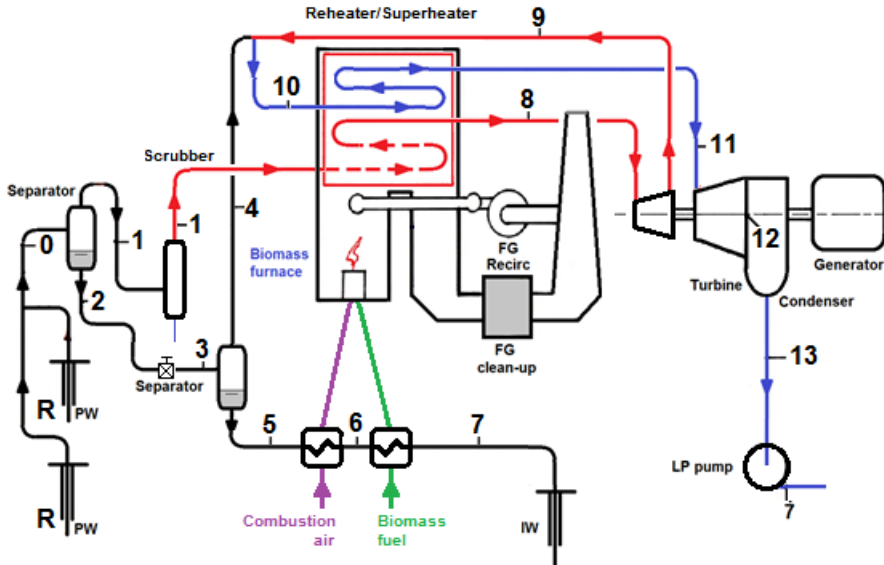
Figure 7: System I - Hybrid geothermal double-flash power plant coupled with a biomass furnace to provide superheat and reheat for the geothermal flash plant.

4.2 System II - Compound Hybrid Geothermal Flash and Biomass Power Plants

System II shown in Figure 8 consists of a geothermal single-flash plant coupled to a biomass plant through, first, the biomass furnace in which the geosteam is superheated before entering its turbine, and second, through a brine heat exchanger that serves as a feed water heater for the biomass plant.
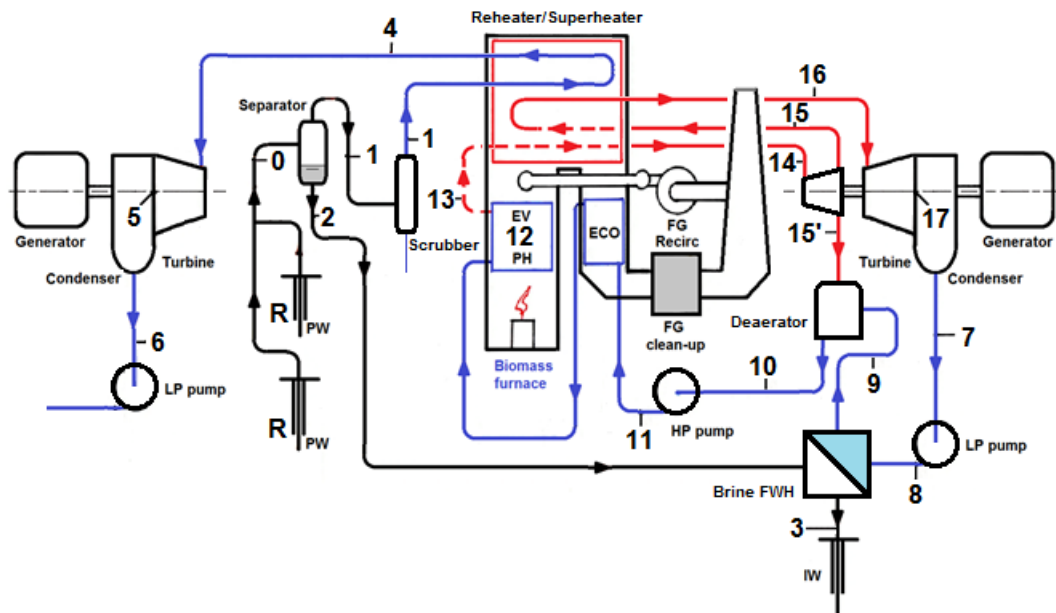
Figure 8: System II - Hybrid biomass power plant integrated with geothermal superheat flash plant.

Adding superheat to the saturated geothermal steam allows for more power output and a drier turbine exhaust relative to a basic single-flash plant. Using the separated brine to provide some of the feed water heating in the biomass plant reduces the amount of steam that must be extracted from the expansion process at state 15' and thereby increases the power output from the biomass plant.

This is a complex system with several adjustable and optimizable design parameters. An optimization was not carried but an analysis for selected values of state-point properties is given in Section 5.

4.3 System III - Geothermal-Enhanced Biomass Power Plant

System III is shown in Figure 9. Here is essentially a dual-pressure biomass power plant in which the low-pressure stream is heated and evaporated in a train of heat exchangers fed with geothermal steam and brine obtained from a nearby geothermal field. The saturated steam from the geothermal evaporator is superheated by passing through the biomass furnace prior to entering the turbine. A throttle valve is shown just ahead of the LP turbine entry point to adjust the LP steam pressure for proper entry into the turbine.
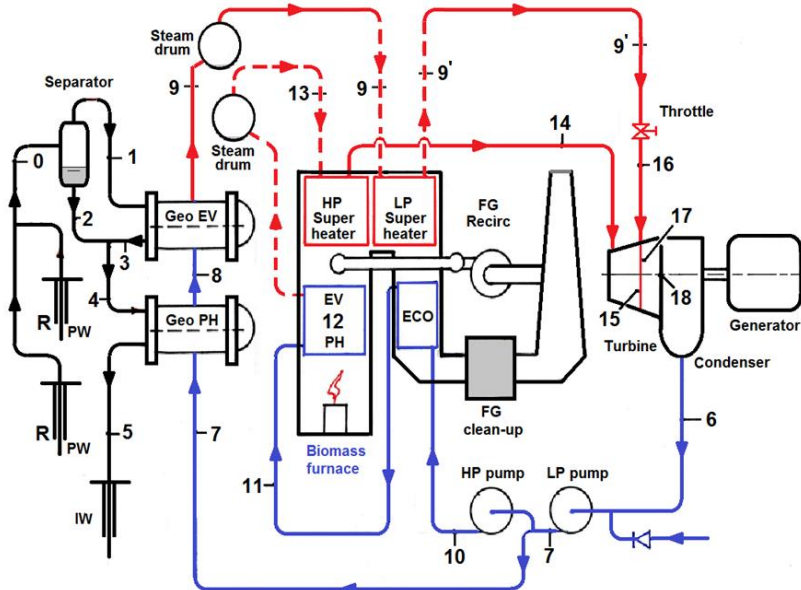
Figure 9: System III - Biomass power plant with geothermal assist for low-pressure steam.

A slight variation of this system, System IIIa, eliminates the LP superheater; the saturated steam from the geothermal evaporator is sent directly to the LP section of the turbine, again through a throttle valve if needed, in a manner very similar to a pass-in, dual-pressure steam turbine in a double-flash plant. However for this case, the steam entering the mixing chamber from the HP section of the turbine is superheated, leading to a superheated steam condition entering the LP stages of the turbine.

System III will produce more power than System IIIa and with less moisture at the turbine exhaust, but it requires a more extensive, complex, and expensive superheater. Simulation studies of these two variations showed that the two are essentially equivalent in terms of thermal efficiency, so only the results for System III are presented in the following section.

5. PERFORMANCE ANALYSIS FOR SYSTEMS I, II AND III

All three systems were analyzed on the assumption that the geofluid has a reservoir temperature of 320°C, typical of the Taupo Volcanic Zone (TVZ). Other parameters were selected as appropriate for each system.

5.1 System I - Biomass-Enhanced Geothermal Double-Flash Plant

The system was modeled using the same methodology as for the Rotokawa example. The simulation demonstrated a strong synergy between the geothermal and biomass energy sources with respect to power output, but the utilization efficiencies are roughly equal. No attempt was made to optimize the system; typical values were selected for all adjustable state-point parameters. Figure 10 shows the processes in temperature-entropy coordinates; Table 3 gives the state-point values. The analysis was performed assuming 100 kg/s of geofluid is produced from the reservoir. The results may be scaled in proportion to the actual flow rate.
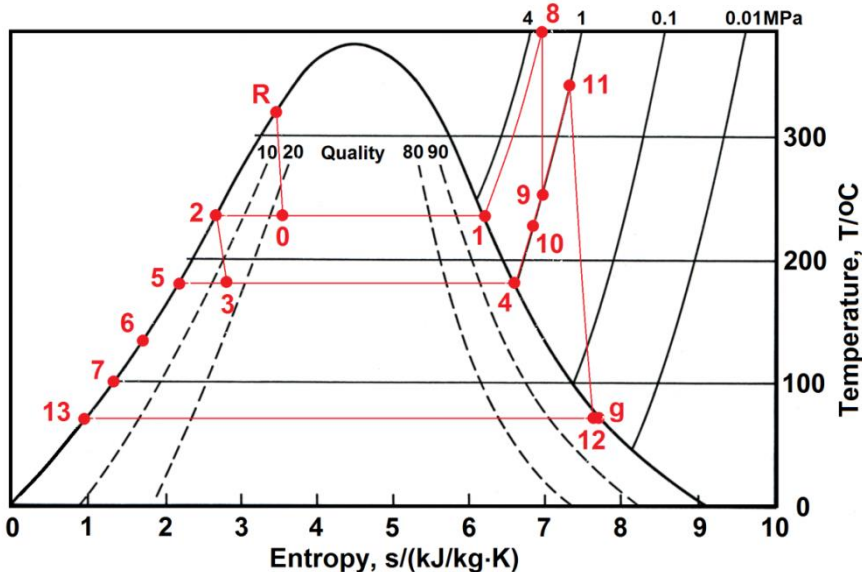
Figure 10: Process diagram for hybrid System I.

Table 3. State-point property values for System I simulation.

	Temp.	Pressure	Entropy	Quality	Enthalpy	Mass flow	Specific Exergy	Exergy
	°C	MPa	kJ/kg·K		kJ/kg	kg/s	kJ/kg	kW
R	**320**	11.280	3.4494	**0**	1462.2	**100**	479.69	47,969
0	**240**	3.3469	3.5295	0.2405	1462.2	100	456.85	45,685
1	240	3.3469	6.1423	1	2803.0	24.054	1052.6	25,320
2	240	3.3469	2.7020	0	1037.6	75.946	268.21	20,370
3	**180**	1.0028	2.7451	0.1363	1037.6	75.946	255.92	19,436
4	180	1.0028	6.5840	1	2777.2	10.352	900.86	9,326
5	180	1.0028	2.1392	0	763.05	65.594	154.15	10,111
6	130	0.2703	1.6346	0	546.38	65.594	81.364	5,337
7	100	0.1014	1.3072	0	419.17	65.594	47.512	3,117
8	400	3.3469	6.8663	SH	3225.8	24.054	1268.96	30,524
9s		1.0028	6.8663		2912.7			
9	257.6	1.0028	6.9566	SH	2959.7	24.054	977.12	23,504
10	232.9	1.0028	6.8507	SH	2904.8	34.406	952.41	32,769
11	350	1.0028	7.3015	SH	3158.1	34.406	1077.17	37,061
12s		0.0312	7.3015		2470.8			
12	70	0.0312	7.6019	0.9776	2573.9	34.406	407.31	14,014
13	70	0.0312	0.9551	0	293.07	34.406	21.805	750
g	70	0.0312	7.7540	1	2626.1			

The hybrid System I was compared to a basic, stand-alone double-flash plant using the same separator and flash conditions; the results are shown in Tables 4 and 5. The incremental thermal efficiency is the ratio of the extra 7,913 kW of power using the hybrid plant over the double-flash plant divided by the biomass heat input. The ideal biomass burn rate is 1.23 kg/s.

Table 4. Summary of heat and work performance for basic and hybrid plants.

Basic Double-Flash Plant		Hybrid System I Plant	
Power Terms, kW			
HP Turbine	4,438	HP Turbine	6,401
LP Turbine	14,150	LP Turbine	20,100
Total Turbines	18,588	Total Turbines	26,501
Heat Input Terms, kWt			
(None)		Superheater	10,170
		Reheater	8,715
		Total Heat Input	18,885
Gross Thermal Efficiencies			
N.A.		0.419 (incremental)	

Table 5. Summary of exergy performance for basic and hybrid plants.

Basic Double-Flash Plant		Hybrid System I Plant	
Exergy Input			
Geofluid - reservoir, kW	47,969	Geofluid - reservoir, kW	47,969
Geofluid - fence, kW	45,685	Geofluid - fence, kW	45,685
		Biomass:	
		Specific exergy, kJ/kg	16,500
		Exergy, kW	20,300
		Total in - reservoir, kW	68,269
		Total in - fence, kW	65,985
Power Output			
Gross electric power, kW	18,588	Gross electric power, kW	26,501
Utilization Efficiencies			
Based on reservoir	0.387	Based on reservoir	0.388
Based on fence	0.407	Based on fence	0.402

The benefit of using the brine as a heating medium for the combustion air and as a drying medium for the wood waste has not been factored into the assessment.

5.2 System II - Compound Hybrid Geothermal Flash and Biomass Power Plants

The parameters chosen for the analysis of System II are based on typical geothermal resource conditions found in the Taupo Volcanic Zone (TVZ) on the North Island of New Zealand, and typical biomass-fueled power plants. For the latter example, the 50 MW Joseph C. McNeil Generating Station in Vermont, U.S. [Burlington, 2013] was examined and pressures and temperatures and flow rates were selected to suit the present needs. The process state-point diagrams for the flash plant and the biomass plant are shown separately in Figures 11 and 12, respectively, to avoid confusion; the numbered state-points are keyed to the flow diagram in Figure 8. Tables 6 and 7 give the state-point properties for the geofluid flash plant and the biomass power plant, respectively.
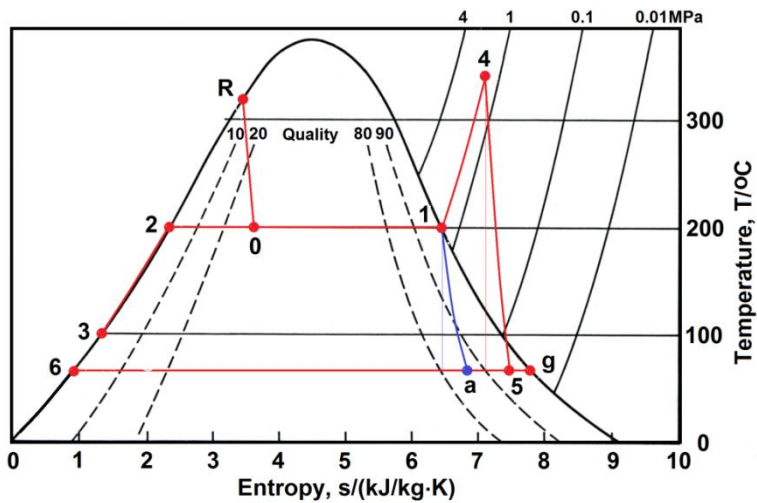
Figure 11: Process diagram for geofluid in System II.
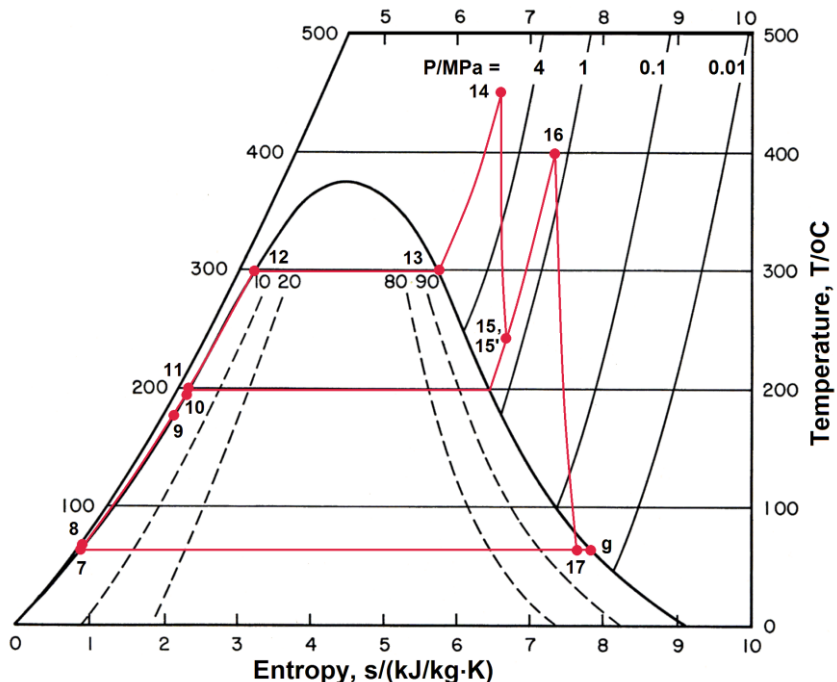
Figure 12: Process diagram for biomass cycle in System II.

Table 6. State-point properties for the geofluid flash plant.

	Temp.	Pressure	Entropy	Quality	Enthalpy	Mass flow	Specific Exergy	Exergy
	°C	MPa	kJ/kgK		kJ/kg	kg/s	kJ/kg	kW
R	**320**	11.2843	3.4494	0	1462.22	**167.607**	479.71	80,402
0	**200**	1.55493	3.6197	0.3145	1462.22	**167.607**	431.17	72,267
1	200	1.55493	6.4302	1	2792.01	52.704	959.54	50,572
2	200	1.55493	2.3305	0	852.27	114.903	188.81	21,695
3	**100**	1.55493	1.3061		420.26	114.903	48.92	5,621
4	350	1.55493	7.0856		3146.92	52.704	1127.54	59,426
5s	70	0.0312	7.0856	0.9017	2396.74			
5	70	0.0312	7.4135	0.9499	2509.27	52.704	396.39	20,891
6	70	0.0312	0.9551	0	293.07	52.704	21.80	1,149
g	70	0.0312	7.7540	1	2626.10			

Table 7. State-point properties for the biomass power plant.

	Temp.	Pressure	Entropy	Quality	Enthalpy	Mass flow
	°C	MPa	kJ/kgK		kJ/kg	kg/s
7	**70**	0.0312	0.9551	0	293.07	48.653
8s	70.1	1.5	0.9551		294.57	
8	70.2	1.5			295.07	48.653
9	**180**	1.5	2.3143	0	763.05	48.653
10	**193**	1.5	2.2639		820.90	48.653
11s	194.0	8	2.2639		828.34	48.653
11	194.6	8	2.2639		830.81	50
12	295.0	8	2.1392	0	1317.31	50
13	295.0	8	5.7450	1	2758.68	50
14	**450**	**8**	6.5579		3273.33	**50**
15'	198.3	1.5			844.56	1.347
15"	198.3	1.5			2790.96	1.347
15s	218.5	1.5	6.5579		2846.24	
15	244.3	1.5	6.6849		2910.30	50
16	**400**	**1.5**	7.2710		3256.47	48.653
17s	70	0.0312	7.2710		2460.34	
17	70	0.0312	7.6190	0.9801	2579.76	48.653

Table 8. Results for geofluid side of hybrid System II.

Mass flow rate from reservoir, kg/s	167.607
Heat input in superheater, kWt	18,705.2
Power output of turbine, kW	33,606.7
Power output of basic 1-flash turbine, kW	25,850.9
Incremental power output, kW	7,755.8
Incremental thermal efficiency	0.415

Table 9. Results for biomass cycle of hybrid System II: 50 kg/s main steam flow.

Hybrid: with geothermal assist	Item	Non-hybrid: No geothermal assist
1.347	*Bleed steam, kg/s*	10.053
	Heat input values, kWt	
24,324.9	Preheater	24,324.9
72,068.6	Evaporator	72,068.6
25732.39	Superheater	25732.39
16842.35	Reheater	13828.47
138,968.3	Total	135,954.4
	Power output values, kW	
18,151.5	High-pressure turbine	18,151.5
32,924.1	Low-pressure turbine	27,032.4
51,075.6	Turbine total	45,184.0
97.42151	Low-pressure pump	79.98829
495.4795	High-pressure pump	495.4795
592.901	Pump total	575.4678
50,482.7	Net power output	44,608.5
0.3633	*Thermal efficiency*	0.3281

Table 10. Summary of exergy performance for basic and hybrid plants.

Basic Single-Flash Plant		Hybrid System II Plant	
Mass flow rates, kg/s			
Geofluid from reservoir	167.61	Biomass	10.27
Exergy Input, kW			
Geofluid: reservoir	80,402	Geofluid: reservoir	80,402
		Biomass	169,486
		Total input	249,889
Power Output, kW			
Geothermal turbine power	25,851	Geothermal turbine power	33,607
		Biomass cycle net power	50,483
		Total System II power	84,090
Utilization Efficiencies			
0.321		0.337	

System III - Geothermal-Enhanced Biomass Power Plant

System III was analyzed for a geothermal resource temperature of 320°C. This is typical for several resources in the Taupo Volcanic Zone (TVZ) on the North Island of New Zealand where there is also an abundant supply of forestry waste products, some close to geothermal resources; see Figure 5 in Section 3. The processes undergone by the working fluids are shown in temperature-entropy coordinates in Figure 13. In the analysis it was assumed that the pressure at states 9 (or 9') and 15 are equal, i.e., the LP-turbine throttle valve is wide open. Initially, the separator temperature of 207°C was arbitrarily chosen for purposes of illustration; later this parameter was optimized to achieve the highest thermal and utilization efficiencies.
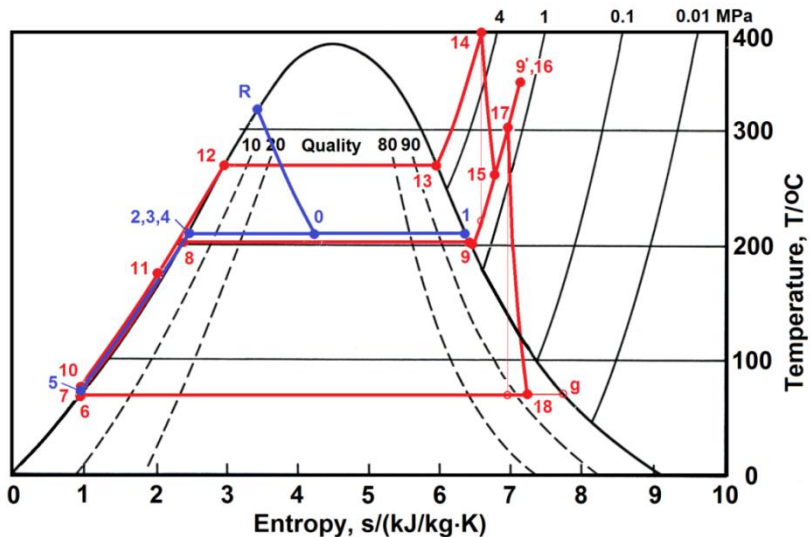

Figure 13: Temperature-entropy process diagram for System III.

Table 11 gives the state-point properties for the geothermal side of the system. Tables 12, 13 and 14 give property information for the biomass side and a summary of the results.

Table 11. State-point property values for geothermal fluid.

	Temp.	Pressure	Entropy	Quality	Enthalpy	Mass flow	Specific Exergy	Exergy
	°C	MPa	kJ/kg·K		kJ/kg	kg/s	kJ/kg	kW
R	**320**	**8.00**	3.4494	0	1317.31	110	293.52	32,287
0	**207**	1.7959	4.2626	0.4687	**1780.00**	**110**	513.77	
1	207	1.7959	6.3783	1	2795.85	51.553	421.25	56,514
2	207	1.7959	2.3964	0	883.96	58.447	92.52	5,407
3	**207**	1.7959	2.3964	0	883.96	51.553	174.13	
4	207	1.7959	2.3964	0	883.96	110	174.13	19,154
5	**70**	1.7959	0.9541	CL	294.51	110		

Table 12. Property values for System III biomass plant working fluid.

	Temp.	Pressure	Entropy	Quality	Enthalpy	Mass flow
	°C	MPa	kJ/kgK		kJ/kg	kg/s
14	**400**	**5**	6.6483	SH	3196.67	48.980
15s		1.5400	6.6483		2897.30	48.980
15	258.42	1.5400	6.7343	SH	2942.21	48.980
9	202.00	1.6210	6.4152	1	2793.18	51.020
9'	**350**	1.5400	7.0904	SH	3147.22	51.020
16	350.00	1.5400	7.0904	SH	3147.22	51.020
17	304.36	1.5400	6.9231	SH	3046.81	100
18s	70.00	0.0312	6.9231		2340.97	
g	70.00	0.0312	7.7540	1	2626.10	
18	70.00	0.0312	7.2316	0.9232	2446.84	100
6	**70**	**0.0312**	0.9551	0	293.07	**100**
7s		1.6210	0.9551	0	294.69	
7	70.17	1.6210	0.9563	CL	295.10	51.020
8	**202**	1.6210	2.3494	0	861.30	51.020
10s		5	0.9563	0	298.55	
10	70.55	5	0.9588	CL	299.41	48.980
11	**167.24**	5	2.0092	CL	709.41	48.980
12	263.94	5	2.9210	0	1154.64	48.980
13	263.94	5	5.9737	1	2794.21	48.980

Table 13. Energy inputs and outputs for System III overall plant.

Turbine & Pump Power Terms					
W-HPT	W-LPT	W-LPP	W-HPP		**W-NET**
kW	kW	kW	kW		**kW**
12,464	59,997	203.2	211.31		**72,046**
Biomass Heat Inputs					
Q-ECON	Q-PH	Q-EV	Q-SH-HP	Q-SH-LP	**Q-IN**
kWt	kWt	kWt	kWt	kWt	**kWt**
20,082	21,807	80,306	19,713	18,063	**159,972**
Geofluid Heat Inputs			**Overall Hybrid Plant**		
Q-PH	Q-EV	**Q-IN**	**W-NET**		**Q-IN**
kWt	kWt	**kWt**	**kW**		**kWt**
28,887	98,564	**127,451**	**71,826**		**287,423**

Table 14. Efficiency results for System III overall plant; numbers in parentheses are based on geofluid properties at the fence.

Thermal efficiency		Utilization efficiency	
Gross	*Net*	*Gross*	*Net*
0.251	0.222	0.322 (0.331)	0.285 (0.293)

The optimization study was a single-parameter optimization performed on System III by varying the separator temperature, T_0, to seek the highest efficiency of the system. Regarding thermal efficiency, two definitions were used: the net power output was compared to (i) the heat added from burning the biomass and (ii) the total heat added from the biomass and from the geofluid. The results showed that there was an optimum choice for T_0 in Case (i) but that in Case (ii) the best efficiency was obtained at the highest separator temperature (or pressure) allowable. The results in Table 15 reveal that there is little variation in the optimum vales of efficiency but the net plant power output depends strongly on the separator conditions; 250°C was arbitrarily chosen as the maximum for the separator. Regarding the utilization efficiency, a similar optimization was carried out; Table 16 gives those results depending on the point of reference for the incoming exergy. The biomass flow rate for all cases is about 11.5-13 kg/s (ideal furnace).

Table 15. Optimized net thermal efficiencies for System III.

	Optimized for Case (i)	Optimized for Case (ii)
Separator temperature, °C	210	250 (max)
(i) Biomass cycle efficiency	0.450	0.437
(ii) Overall plant efficiency	0.252	0.269
Net plant power output, kW	69,983	74,404
Biomass flow rate, kg/s	11.66	12.75

Table 16. Optimized net utilization efficiencies for System III.

	Based on reservoir	Based on fence
Separator temperature, °C	219	222
Overall plant	0.312	0.321
Net plant power output, kW	71,312	71,638
Biomass flow rate, kg/s	11.90	11.96

6. ENGINEERING CHALLENGES

There are some engineering challenges facing the designer of the hybrid systems proposed in this paper, Systems I, II and III.

Wherever geothermal steam is being superheated, the issue arises of corrosion due to the presence of hydrogen sulfide, H_2S, in the steam. Both Systems I and II would be subject to this problem. One way to avert this problem is to remove the H_2S and other noncondensable gases (NCG) upstream of the furnace. A condenser-vent-reboiler might be able to accomplish this and provide clean steam to the superheater. Otherwise, the tube material for the superheater would have to be carefully selected to withstand the sour gas and maintain strength under high temperature conditions, especially when the geosteam is at high pressure as is often the case for geothermal resources in the Taupo Volcanic Zone (TVZ) of New Zealand.

Since steam contacts the inside of the superheater tubes, the wall temperature of some of the tubes will be close to the flue gas temperature, up to 900-1000°C. Flue gas attemperation to limit superheater tube metal temperatures to around 650°C is desirable to avoid tube burn out and associated material creep failure problems. The sour gas problem in System I will be mainly in the high-pressure steam superheater since the bulk of the NCG will be released in the first separator, leaving the low-pressure line relatively NCG-free. However, because the HP steam is mixed with the LP steam prior to the reheater, NCGs will be present but at lower concentration and at lower temperatures.

Reducing the flue gas temperatures to better match the requirements of the hybrid system using exhaust gas recirculation would alleviate these problems. However, there are no known commercial systems to handle the type fluids that would be encountered in these novel designs, making research and development necessary to achieve a successful plant.

In both System I and II, liquid carry-over from the separators can be a problem and will require effective scrubbers to maintain good steam conditions for the heaters and the turbine.

System II, like System I, might face a problem from potential superheater metallurgical problems as just described, however, because this system uses basically a conventional biomass furnace, there should be no special problems with attemperating the combustion flue gases.

System II might suffer from scaling in the brine feed water heater, but this is no different from the situation in a bottoming binary plant. Scaling can be avoided by careful choice of temperature and/or controlled through the use of scale-control chemicals.

System III is fundamentally a biomass power plant with geothermal augmentation and as such avoids all the above-mentioned issues. The geothermal fluid is used in a way that is similar to binary plants except that the geofluid transfers heat to clean, demineralized water in the closed biomass cycle rather than a low-boiling point working fluid. Scaling might occur in the lowest temperature sections of the preheater but this can be averted as described above.

Either variation eliminates the aforementioned problems with the furnace since conventional biomass furnace technology would be used and the cycle working fluid is clean water, the geofluids being used solely as heating media.

Besides these engineering challenges, the hybrid concepts can be feasible only if the geothermal resource is located close enough to the forest residue supply to make the venture economically feasible.

7. CONCLUDING REMARKS

Never before in the field of human endeavor has there been so crucial a time when mankind must strive to achieve a sustainable and renewable energy future. The hybrid concept presented here synergistically links the power generation capabilities of two renewable power resources – geothermal and biomass – so as to achieve greater power output than would be possible if the two plants operated on an individual stand-alone basis.

Thain and DiPippo

This paper demonstrates that the hybridization can be achieved in a variety of ways to best match the characteristics of the energy sources. Relative to the base geothermal plant, the hypothetical hybridization of the Rotokawa I power plant resulted in a gain of 8,548 kW or 32% more net power, while the exergy utilization efficiency was comparable but somewhat lower because of the large temperature difference in the biomass superheater.

8. ACKNOWLEGEMENTS

REFERENCES

Bruce, A.W., Engineering Aspects of a Geothermal Power Plant, *Geothermics – Special Issue 2*, *Proc. U.N. Symp. Development and Utilization of Geothermal Resources*, **2**, Pt. 2, Pisa (1970) 1516-1520.

Burlington, Joseph C. McNeil Generating Station, Burlington (Vermont) Electric Department (2013): https://www.burlingtonelectric.com/page.php?pid=80&name=mcneil_facts

Ciolkosz, D., Characteristics of Biomass as a Heating Fuel, *Renewable and Alternative Energy Fact Sheet*, Code # UB043, College of Agricultural Sciences, The Pennsylvania State University (2010) 1-2.

Dias, R.A., Perrella B., J.A., Energetic and Exergetic Analysis in a Firewood Boiler, *Revista de Ciência & Tecnologia*, **12**, No. 23 (2004) 15-24.

DiPippo, R., An Analysis of an Early Hybrid Fossil-Geothermal Power Plant Proposal, *Geothermal Energy Magazine*, **6** (March 1978) 31-36.

DiPippo, R, Marcille, D.F., Exergy Analysis of Geothermal Power Plants, *Geothermal Resources Council TRANS*., **8** (1984) 47-52.

DiPippo, R, Avelar, E.M., Compound Hybrid Geothermal-Fossil Power Plants, *Geothermal Resources Council TRANS*., **3** (1979) 165-168.

DiPippo, R., Khalifa, H.E., Correia, R.J., Kestin, J., Fossil Superheating in Geothermal Steam Power Plants, *Geothermal Energy Magazine*, **7** (Jan. 1979) 17-23.

DiPippo, R., *Geothermal Power Plants, 3rd. Ed.: Principles, Applications, Case Studies and Environmental Impact*, R. DiPippo, Chap. 5, Single-Flash Steam Power Plant, Butterworth-Heinemann: Elsevier, Oxford, England (2012a).

DiPippo, R., *Geothermal Power Plants, 3rd. Ed.: Principles, Applications, Case Studies and Environmental Impact*, R. DiPippo, Chap. 10, Exergy Analysis Applied to Geothermal Power Systems, Butterworth-Heinemann: Elsevier, Oxford, England (2012b).

ENEL, Stillwater Solar Geothermal Hybrid Project (2011): http://www.enelgreenpower.com/en-GB/ena/power_plants/wm/Stillwater_Solar/

Geothermal Hot Line, Honey Lake Power Facility under Construction, **18**, No. 2 (1988) 61-62.

Hansen, A., Thermal Cycles for Geothermal Sites and Turbine Installation at The Geysers Power Plant, California, *Proc. New Sources of Energy*, **3** *Geothermal Energy: II*, United Nations, Rome (1961) 365-379.

James, C.R., Superheating of Geothermal Steam for Power, *New Zealand Engineering*, **25**, No. 12 (1970) 325-330: http://search.informit.com.au/documentSummary;dn=023914344329281;res=IELENG

Kaingaroa Timberlands, Kaingaroa Forest, Rotorua, New Zealand (2013): http://www.kaingaroatimberlands.co.nz/default.htm

Kestin, J., DiPippo, R., Khalifa, H.E., Hybrid Geothermal-Fossil Power Plants, *Mechanical Engineering*, **100** (Dec. 1978) 28-35.

Khalifa, H.E., DiPippo, R., Kestin, J., Geothermal Preheating in Fossil-Fired Steam Power Plants, *Proc. 13th Intersociety Energy Conversion Engineering Conference*, **2** (1978) 1068-1073.

Legmann, H., Rotokawa Geothermal Combined-cycle Power Plant, *Bulletin d'Hydrogiologie*, No. I7, Centre d'Hydrogiologie, Universid de Neuchritel (1999) 425-431.

Lind, L., Mroczek, S., Bell, J., Energy Efficient – Rotokawa Geothermal Power Station, *Case Study 15*, Wairakei Research Centre, Taupo, New Zealand (2013).

Manente, G., Field, R., DiPippo, R., Tester, J.W, Paci, M., Rossi, N., Hybrid Solar-Geothermal Power Generation to Increase the Energy Production from a Binary Geothermal Plant, *Proc. 2011 ASME International Mechanical Engineering Congress and Exposition*, Paper No. IMECE 2011-63665 (2011) Denver, Colorado, USA.

McKinnon, M., Volcanic Plateau places - Kāingaroa to Kaimanawa, *Te Ara - The Encyclopedia of New Zealand*, updated November 14, 2012: http://www.TeAra.govt.nz/en/map/15074/kaingaroa-to-kaimanawa

Moran, M.J., *Availability Analysis: A Guide to Efficient Energy Use* (Corrected Edition), ASME Press, New York (1989).

Morrison-Knudsen, Engineering and Economic Study Report, Vol. I, Executive Summary - Honey Lake Hybrid Power Plant Project, Morrison-Knudsen Company, Inc. and International Engineering Company, Inc. (March 1982).

NIST, Nat. Inst. of Standards and Technology Standard Reference Database 23, NIST Reference Fluid Thermodynamic and Transport Properties Database (REFPROP), Ver. 9.1 (2013): http://www.nist.gov/srd/nist23.cfm

NZCEC, Greater Wellington Regional Council Forest Residue Utilisation Trial - Final Report, New Zealand Clean Energy Centre, June 19 (2009).

Roche, M, Exotic forestry - Forestry in the 1800s, *Te Ara - The Encyclopedia of New Zealand*, July 13 (2012): http://www.TeAra.govt.nz/en/exotic-forestry/

Wall, G., EOLSS; National Exergy Accounting of Natural Resources, *Exergy, Energy System Analysis and Optimization*, Vol. III, C.A. Frangopoulos, Ed., *Encyclopedia of Life Support Systems (EOLSS)* (Undated).

Wikipedia, Kaingaroa Forest (2013): http://en.wikipedia.org/wiki/Kaingaroa_Forest

X-Rates, Currency Exchange Rates, 2009: http://www.x-rates.com/average/?from=NZD&to=USD&amount=1.00&year=2009